RESEARCH PAPER

PCCP
www.rsc.org/pccp

Vibrational dissipation and dephasing of $I_2(v = 1–19)$ in solid Kr

Michael Karavitis, Takayuki Kumada, Ilya U. Goldschleger and V. Ara Apkarian*

Department of Chemistry, University of California, Irvine, CA, 92697-2025, USA

Received 19th October 2004, Accepted 18th January 2005
First published as an Advance Article on the web 1st February 2005

Time- and frequency-resolved coherent anti-Stokes Raman scattering is used to carry out systematic measurements of vibrational dephasing on $I_2(v = 1–19)$ isolated in solid Kr, as a function of temperature, $T = 7–45$ K. The observed quantum beats, $\omega_{v',v''}$ allow an accurate reconstruction of the solvated molecular potential, which is well represented by the Morse form: $\omega_e = 211.56 \pm 0.14$, $\omega_e x_e = 0.658 \pm 0.006$. Near $T = 7$ K, the coherence decay rates $\gamma_{v,0}$ become independent of temperature and show a linear v-dependence, indicative of dissipation, which must be accompanied by the simultaneous creation of at least four phonons. At higher temperatures, the T-dependence is exponential and the v-dependence is quadratic, characteristic of pure dephasing *via* pseudo-local phonons. A normal mode analysis suggests librations as the principle modes responsible for pure dephasing.

1. Introduction

Vibrational phase and energy transfer in condensed media, in the liquid phase[1,2] and in the solid state,[3] are fundamental building blocks of many-body dynamics. The more modern treatments of the subject aim at non-perturbative,[4,5] and explicit accounting of the many-body quantum dynamics of realistic systems,[6–8] the prototype being a Morse oscillator coupled to various types of baths.[9] While earlier critical analyses of the process were based on frequency-domain linewidth data,[3] the advent of short pulse sources has enabled direct time domain scrutiny,[10–12] time-resolved coherent anti-Stokes Raman (TRCARS) scattering,[13–16] being one of the many informative nonlinear spectroscopic tools.[17] The database nevertheless remains limited to studies of fundamentals and first overtones, the more complete vibration-dependent studies being limited to such systems as CO,[18] NO,[19] isolated in rare gas matrices, where the relaxation rates are slow enough to enable time-resolved studies that rely on detector speed. Using electronically resonant TRCARS we, report measurements as a function of excitation amplitude, v, and bath temperature, T, on the prototypical system of molecular iodine isolated in solid Kr. Given the well defined structure and interaction potentials of this system, we expect the data to be valuable for rigorous tests of theories on vibrational dephasing and dissipation in the solid state. The experimental method was initially implemented in Ar matrices,[20] with limited success due to limitations imposed by multi-photon induced dissociation of the molecule.[21] This consideration is unimportant in solid Kr, as established in our TRCARS investigation of the low-lying vibrations.[22] Here, we report measurements on vibrational levels up to $v = 19$, as a function of temperature, $T = 7–45$ K. The upper limit in v is imposed by laser-induced fluorescence from the ion-pair states, which overwhelms the TRCARS signal. The upper limit in temperature corresponds to the onset of self-diffusion in solid Kr, which leads to signal degradation during the measurements. Although the lower temperature limit is dictated by the cryostat employed, the data allow extrapolation to $T \rightarrow 0$. In a follow-up study by Pettersson *et al.*, the low temperature limit of measurements is extended to 2 K.[23]

2. Experimental

The measurements are carried out on thin films of I_2 isolated in solid Kr, at a dilution ratio of 1 : 5000. Krypton gas of stated purity 99.995% (Air Gas) was used without further purification. Iodine of stated purity 99.99 + (Aldrich Chemicals) was subjected to three freeze–pump–thaw cycles prior to use. Matrices of high optical quality are obtained on a sapphire substrate held at 35 K, by pulsed deposition of the premixed gas from a 1 l bulb, at bulb pressures ranging from 500 torr to 1000 torr. The films, at an estimated thickness of $\sim$100 μm, appear purple to the eye.

The excitation pulses are derived from two home-built non-collinear optical parametric amplifiers (NOPA) pumped by a commercial laser (Clark-MXR 2001): $\lambda = 775$ nm, 1 mJ pulse^{-1}, 1 kHz repetition rate. Save for small variations, the NOPA design follows that described by Riedle.[24,25] In its standard configuration, the NOPA generates $\sim$800 cm^{-1} bandwidth, compressible to 1.5× transform limit using a pair of SF10 prisms. To reduce the bandwidth, the white-light continuum seed is pre-stretched using a 3 cm-long optical flat made of SF10 glass. This arrangement yields pulses of $\sim$100 fs, at a bandwidth of 350 cm^{-1}. Three non-collinear beams are used. The output of one of the NOPAs is split to provide pump and probe beams, while the second NOPA provides the Stokes beam. Delay lines control the timing between the three pulses. The three beams are brought to focus on the sample using a single achromat (fl = 200 mm). The experimental four-wave coherence length is 500 μm, as determined by monitoring CARS generated from a translating thin glass plate.

The CARS beam is spatially filtered using an iris pinhole, and spectrally filtered using a 1/4-monochromator (McPherson, 218). The signal is detected using a cooled photomultiplier, averaged using a boxcar integrator, digitized, and then stored on a personal computer for further analysis. The data is acquired during continuous scan of the delay line, while simultaneously recording the interferogram of a tracer He:Ne laser as an absolute time base. This arrangement is effective in eliminating all frequency modulations (FM) caused by mechanical imperfections. However, amplitude modulations (AM) may persist. In our prior report on TRCARS in Kr, a sharp AM signal at 42 cm^{-1} was observed and was tentatively analyzed as signal.[22] We have since verified that this AM was generated by one of the translation stages, and have corrected the fault.

3. Results and analysis

The measurements are restricted to the $P^{(0,3)}$ component of the molecular third-order polarization, in which the three input

DOI: 10.1039/b416143b

pulses act on the state ket (bra) while the bra (ket) evolves field free.[20] With coincident pump (P) and Stokes (S) pulses that are resonant with the electronic X $\leftrightarrow$ B transition of molecular iodine, a second-order wavepacket (Raman packet) is prepared as a vibrational superposition on the ground electronic state:

$$|\varphi^{(2)}\rangle = \sum_v a_v|v\rangle.$$

The vibrational coherence, which is created as a spatial grating formed by the non-collinear P- and S-pulses, decays as it evolves. The evolving coherence is probed with a time-delayed copy of the P-pulse. The action of the probe pulse (Pr), and the anti-Stokes radiation detected through a spectral filter, can be reduced to the projective measurement of the evolving coherence, which in the frequency integrated mode of detection, reduces the observable signal to damped sinusoids:[22]

$$S(t) \propto \sum_{v,v\prime} 2c_v c_{v\prime} f(\omega) \cos[\omega_{v,v\prime}t + \phi_{v,v\prime}] \exp[-(\gamma_v + \gamma_{v\prime})t] \quad (1)$$

The coefficients, c_v, are determined by the spectral composition of the pump and Stokes pulses, and the detection bandpass; $f(\omega)$ is the experimental frequency response due to the finite widths of the laser pulses; $\omega_{v,v\prime} = \omega_v - \omega_{v\prime}$ are the beat frequencies between the prepared vibrations; and $\gamma_v \equiv \gamma_{v,0}$ is the overall rate of decay of amplitude correlation between state v and $v = 0$. The reproduction of the signal in terms of eqn. (1) suggests the decomposition of the coherence decay in terms of constituent vibrational amplituides

$$|\varphi^{(2)}(\vec{k}_P - \vec{k}_S, t)\rangle\langle\varphi^{(0)}(t)| = \exp[i(\vec{k}_P - \vec{k}_S)\vec{r}] \sum_v a_v \exp[-\gamma_{v,0}t - i(E_v - E_0)t/\hbar]|v\rangle\langle 0| \exp[iE_0 t/\hbar] \quad (2)$$

The information sought in these measurements are: (a) the beat frequencies, to reconstruct the solvated X-state potential; (b) the γ_v dephasing times associated with individual vibrational states.

At low temperatures and for low-lying vibrations, the coherences are sufficiently long-lived to show nodal patterns above the fundamental beats, as illustrated in Fig. 1. In frequency domain, this simply implies that the spectral components are well-resolved, *i.e.,* the spectral width associated with a given beat is narrower than the anharmonic splitting between beats. As long as this condition prevails, broad-band measurements are gainful since a single measurement yields all of the sought parameters for the entire superposition. This was demonstrated for the $v = 1$–6 superposition in our prior report.[22] In contrast, when the decay time is too short to allow the development of nodes, or equivalently, if the spectral components are not resolved, then the extraction of state specific information becomes unreliable. It is necessary to reduce the laser bandwidth, ideally to prepare a two-state superposition (single beat) in a given measurement, even though this necessitates measurements at many different Stokes shifts. The data set to be presented was obtained using many colors, with bandwidths adjusted to resolve state specific information. In the long-lived coherences, the spectrally resolved components are individually fitted, and the parameters are optimized from the reconstructed signal in time and frequency domain. With the reduced bandwidth measurements, the most reliable dephasing data is obtained by fitting the zero-frequency component in eqn. (1), and invariably, this can be well represented by a single exponential decay.

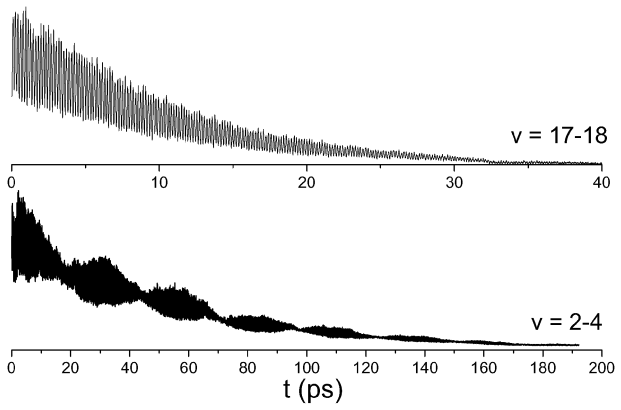

Fig. 1 Time resolved CARS signals for $v = 2,3,4$ and $v = 17,18$ superpositions, obtained at 7 K. Single exponential decay times of the two superpositions are 52 ps and 12 ps, respectively.

We have also collected frequency resolved TRCARS data, by recording the entire CARS spectrum at a given probe delay, as illustrated in Fig. 2. Such data is valuable to test the possibility of coherent dissipation, which would appear as a skewing of the spectrum as a function of time; or for establishing whether different members of the packet decay at different rates, which would develop asymmetry between the blue and red edges of the spectrum with time. Although only a segment of the time record is shown for clarity, within the sensitivity of detection, the time dependent spectra simply decay symmetrically: population relaxation proceeds with random phase. As illustrated in Fig. 2, the two-dimensional data set can be decomposed in terms of contributing beats in frequency domain. Within the spectral resolution dictated by the decay times, the widths of the spectral components are nearly identical. It would seem that the entire packet decays at a fixed rate. A non-parametric extraction of v-dependent decoherence time is only obtained by preparing excitations centered on different vibrations, otherwise, in the analysis of broad superpositions we impose a virial expansion of $\gamma(v)$.[22]

The Birge–Sponer plot obtained from the beat frequencies, is shown in Fig. 3. The data may be fitted to include cubic anharmonicity:

$$\omega_{v+1,v} = \omega_e - 2\omega_e x_e(v + 1) + 3\omega_e y_e(v^2 + v + 13/12) \quad (3a)$$

However, in such a fit the error bar associated with $\omega_e y_e$ is larger than its magnitude, lending it indeterminate. The fit shown in Fig. 3 is restricted to only the first anharmonicity, yielding

$$\omega_e = 211.56 \pm 0.14 \text{ cm}^{-1}, \omega_e x_e = 0.658 \pm 0.006 \text{ cm}^{-1} \quad (3b)$$

The parameters extracted with this expanded set of vibrational states are within experimental error of the prior determination, which was based on a single measurement of the $v = 1$–6 superposition.[22] In effect, the solvated potential up to $v = 19$ is adequately described by the Morse form.

The temperature dependent dephasing rates of beats between states $v = 7$–8, $v = 13$–14 and $v = 17$–18 are shown in Fig. 4. The data between $T = 7$ K and $T = 40$ K can be fit to the exponential form $\gamma(T) = A + B\exp(-\theta/T)$. This is quite generally diagnostic of dephasing by pseudo-local phonons,[3] which can also be reduced down to the exchange model of Harris,[26,27] and the scattering of uncorrelated phonons by de Bree and Wiersma.[28] Above $T = 40$ K, which marks the onset of self-diffusion of the host, the data is not very reliable, since the signal amplitude decays during measurements. Near $T = 7$ K, dephasing times reach a T-independent plateau. A plot of the vibration dependence of the rates at $T = 7$ K and at $T = 34$ K is shown in Fig. 5. While the T-independent dephasing rates show a linear dependence on v, the high temperature rates show a quadratic dependence. Note, the very long-lived states $v \leqslant 3$ deviate from the quadratic fit. In this limit, inhomogeneous contributions become significant, as evidenced by

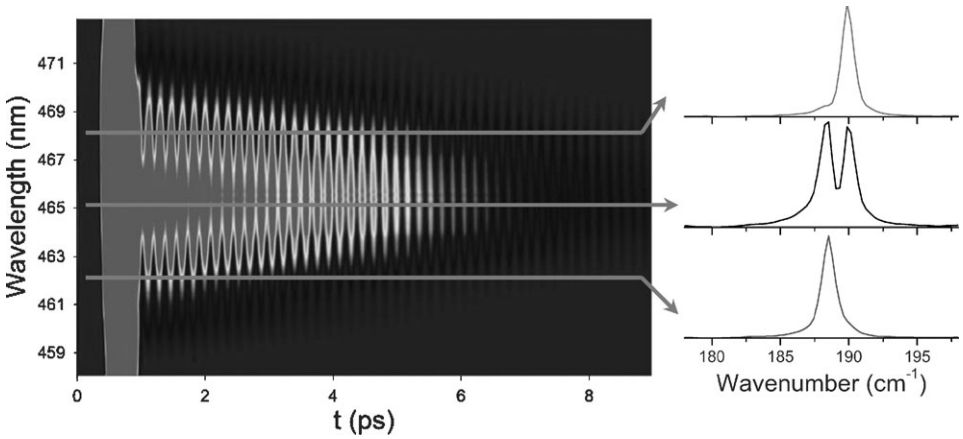

Fig. 2 Time and frequency resolved CARS signal for the $v = 16,17,18$ superposition. The FFT spectra along the indicated optical frequency slices are shown. Although the time resolution is sufficient to clearly distinguish the anharmonically shifted $\omega_{17,16}$ and $\omega_{18,17}$ beats, the frequency resolution is not sufficient to distinguish the widths of the component beats. The symmetric temporal decay of the 2D spectrum reinforces this, and establishes the absence of coherent dissipation.

variation of the extracted decay times from sample-to-sample. Otherwise, the entire data set, T and $v < 3$ deviate from the quadratic fit. In this limit, inhomogeneous contributions become significant, as evidenced by variation of the extracted decay times from sample-to-sample. Otherwise, the entire data set, T and v dependence, can be represented by the single formula:

$$\gamma(v,T) = \frac{v}{\tau_1} + \frac{v^2}{\tau_2} e^{-\vartheta/T} \qquad (4a)$$

with

$$\tau_1 = 350 \pm 12 \text{ ps}, \tau_2 = 330 \pm 33 \text{ ps}, \theta = 65 \pm 4 \text{ K} \qquad (4b)$$

Eqn. (4a) divides the observed dephasing rates into a T-independent term, which has linear v-dependence, and a quadratic v-dependent term, which has exponential T-dependence, characteristic of an activated process. The T-dependence can also be well fit assuming that the activation is that of the thermal occupation of a phonon:

$$\gamma(v,T) = \frac{v}{\tau_1} + \frac{v^2}{\tau_2} \frac{1}{e^{\vartheta/T} - 1} \qquad (5a)$$

with

$$\tau_1 = 355 \pm 10 \text{ ps}, \tau_2 = 560 \pm 70 \text{ ps}, \theta = 54 \pm 4 \text{ K} \qquad (5b)$$

While without the incorporation of the phonon density of states this form is not very meaningful, we include it here to show that the extracted value of θ is highly model-dependent, and both eqns. (4) and (5) should simply be regarded as formulae that can be used to summarize the data set within its accuracy.

4. Discussion

In the range of the measurements, up to $v = 19$ ($E \sim 3500$ cm^{-1}), I_2 isolated in Kr is well represented as a Morse oscillator in a van der Waals solid. Solvation reduces the harmonic frequency to $\omega_e = 211.56$ cm^{-1} from its gas phase value[29] of 214.57 cm^{-1}, and increases the anharmonicity to $\omega_e x_e = 0.658$ cm^{-1} from its gas phase value of $\omega_e x_e = 0.6127$ cm^{-1} (in Ar,[21] $\omega_e = 214.0$ cm^{-1}, $\omega_e x_e = 0.638$ cm^{-1}). This is consistent with the occupation of a bi-substitutional site,[30] which is somewhat looser in Kr than in the equivalent cavity in Ar, such that the molecule is subject to tensile stress. Given the symmetry of the trapping site, the local potential can be expected to be limited to an expansion in even powers of the molecular intermolecular coodinate, q. Then the lowest order term, $k'q^2/2$, can be extracted from the shift in the harmonic frequency of the molecule:$\omega_e^2(s) - \omega_e^2(g) = k'/\mu$. Inclusion of this local quadratic potential, $V(q) = V_g - k'q^2/2$, in which V_g is the gas phase potential of $I_2(X)$ and $k' = 2.27 \times 10^3$ cm^{-1} Å^{-2}, fully accounts for the observed increase in the anharmonicity. The effect of the quartic term is not discernible in the energy range of the measurements. In Fourier transformed TRCARS spectra of long-lived vibrational coherences, there is evidence that a minority of the molecules, ~1%, is trapped near defect sites. The resulting spectra are in good agreement with a model that assumes vacancy point defects.[31] The

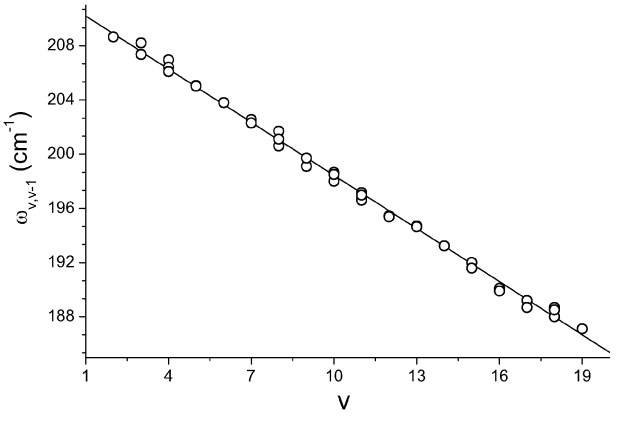

Fig. 3 Birge–Sponer plot of the observed beat frequencies. The linear fit to the slope and intercept yield: $\omega_e = 211.56 \pm 0.14$ cm^{-1}, $\omega_e x_e = 0.658 \pm 0.006$ cm^{-1}: the solvated potential is well represented as a Morse curve.

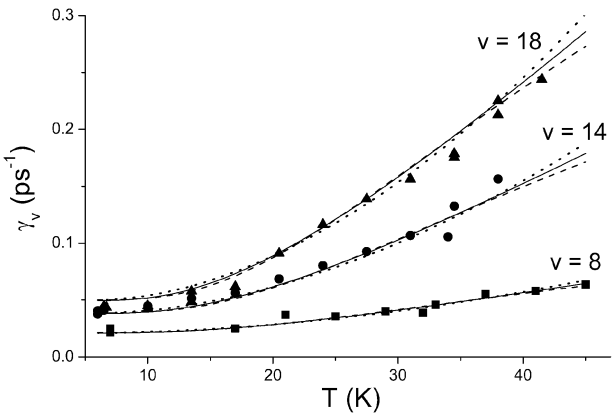

Fig. 4 Temperature dependence of the dephasing rates, $\gamma(v,T)$ for $v = 8$ (■), 14 (●) and 18 (▲). The dashed lines are the analytical fits to eqns (4)–(6).

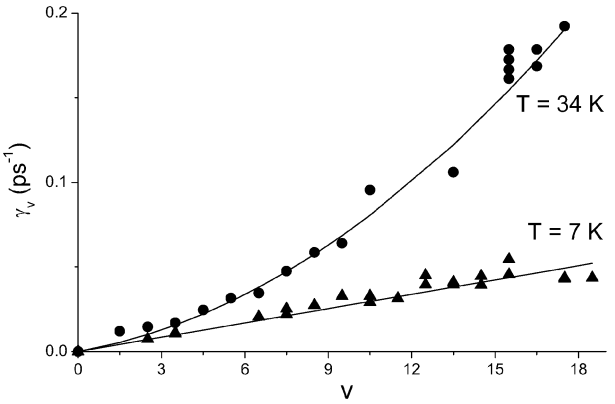

Fig. 5 Vibration dependence of the observed dephasing rates at $T = 7$ K (▲) and $T = 34$ K (●). Solid lines are analytical curves corresponding to the global best fits to $\gamma(v,T)$ – linear at 7 K and quadratic at 34 K.

reported phase and population transfer rates are strictly for molecules trapped in the principal isolation site.

The observation of coherence decay rates that are much longer than characteristic periods of motion of the lattice or molecule; or equivalently, the presence of a sharp Raman spectrum, implies a system weakly coupled to its environment:

$$H = H_S(q,p) + H_B(\boldsymbol{Q},\boldsymbol{P}) + H_{SB}(q,p,\boldsymbol{Q},\boldsymbol{P}) \tag{6}$$

in which q,p represent the molecular coordinates, while $\boldsymbol{Q},\boldsymbol{P}$ represent the set of normal coordinates of the lattice phonons. It is then useful to carry out the discussion in terms of the uncoupled basis set:

$$|v,\{n_i\}\rangle = |v\rangle \prod_i |n_i\rangle \tag{7}$$

where $|v\rangle$ represent the eigenstates of the solvated Morse oscillator:

$$\begin{aligned} H_S &= -\frac{\hbar^2}{2\mu}\frac{d^2}{dq^2} + D(1-e^{-\beta q})^2 \\ &= \frac{\hbar\omega_e N}{2(N+1)}(b^\dagger b + bb^\dagger) + \frac{\hbar\omega_e}{4(N+1)} \end{aligned} \tag{8}$$

and $|n_i\rangle$ represent eigenstates of the normal modes of the doped solid, Q_i, which at the cryogenic temperatures of interest may be treated as harmonic:

$$\begin{aligned} H_B &= \sum_i \left(-\frac{\hbar^2}{2M_i}\frac{d^2}{dQ_i^2} + \frac{1}{2}M_i\omega_i^2 Q_i^2\right) \\ &= \sum_i \hbar\omega_i(a_i a_i^\dagger + 1/2) \end{aligned} \tag{9}$$

The observed v,T-dependent measurements of dephasing then allow the characterization of the effective system–bath interaction. Assuming a potential coupling given as an expansion:

$$V_{SB}(q,\boldsymbol{Q}) = qf(Q) + q^2 g(Q) + \cdots \tag{10}$$

mechanistic associations with a given expansion term can be made by noting that for a harmonic phonon:

$$Q = \frac{\hbar k}{2\omega}(a + a^\dagger) \tag{11}$$

while for the quantum Morse oscillator:[32]

$$q \approx \sqrt{\frac{\hbar}{2\mu\omega}}[(b+b^\dagger) + \sqrt{x_e}(b+b^\dagger)^2] \tag{12}$$

where x_e is the anharmonicity coefficient, and $a,a^\dagger$ and $b,b^\dagger$ are the annihilation and creation operators.

The observation of a linear v-dependent coherence decay in the $T \to 0$ limit uniquely identifies the process as dissipation, which at the cryogenic temperatures of relevance is dominated by the population relaxation $v \to v-1$ with rate $k_{v\to v-1} = 2\gamma_v \propto |\langle v'|b|v\rangle|^2 = v\delta_{v-1,v'}$. This process may only be driven by the linear term in the system–bath coupling, $qf(Q)$. To conserve energy, the process must be accompanied by the creation of minimally four phonons. We are lead to conclude that to the lowest order, dissipation in this system is driven *via* the quintic coupling: $qf(Q) = \lambda_{i,j,k,l}^{(1,4)} qQ_iQ_jQ_kQ_l$ where the superscript on the expansion coefficient identifies the order of coupling to the system and bath coordinates.

Dephasing processes that consist of scattering of phonons with preservation of the vibrational state of the molecule, to lowest order, must be limited to the number operator along the molecular coordinate: $bb^\dagger + b^\dagger b$. For a Morse oscillator, this can be induced either *via* the internal anharmonicity, $\sqrt{x_e}(b + b^\dagger)^2$ term in eqn. (12), in which case the coupling is linear in the system coordinate, q. Alternatively, dephasing can be induced *via* intermolecular anharmonicity which is quadratic in the system coordinate, q^2. In either case, a quadratic v-dependence would arise, as observed in the high temperature decay of the vibrational coherence. The requirement of tracing over the bath implies that only even powers of the coupling along phonon coordinates may contribute,[33] therefore to lowest order, dephasing *via* intramolecular anharmonicity is driven by the cubic term $\lambda^{(1,2)}qQ^2$, while the intermolecular anharmonic term is quartic, $\lambda^{(2,2)}q^2Q^2$. The experiment does not distinguish between these two mechanisms.

The exponential temperature dependence of dephasing suggests an activated process, rather than the Debye density of states, which would predict a T^7 dependence[34]—particular phonons that are subject to an energy gap are involved. For phonons sharply peaked at ω_k, the requisite Q^2 dependence *via* $a^\dagger a$ operator would predict a temperature dependence $\gamma(T)\alpha$ $n(\omega_k)[n\omega_k) + 1]$, where $n(\omega_k) = 1/[\exp(\hbar\omega_k/kT) - 1]$ is the phonon occupation number. As shown in Fig. 4, the data can be well fit to this expectation:

$$\gamma(T) = \frac{v}{\tau_1} + \frac{v^2}{\tau_2} n(\omega_k)[n(\omega_k)+1] \tag{13a}$$

with

$$\begin{aligned} &\tau_1 = 353 \pm 16 \text{ ps}, \tau_2 = 1550 \pm 800 \text{ ps}, \\ &\omega_k = 27 \pm 6 \text{ cm}^{-1} \text{ or } \theta_k = 40 \pm 10 \text{ K} \end{aligned} \tag{13b}$$

Note, the exponential fit in eqn. (5) yields a phonon frequency of 45 ± 3 cm^{-1}. The data does not favor either of these limiting models. Rather than a single phonon, the decay may be ascribed to a spectral density of phonons, for which we consider the likely modes.

We carry out a normal mode analysis on a cell of 108 Kr atoms containing a single I_2 molecule as a bi-substitutional dopant. Pair potentials are used, and the normal modes are computed after simulated annealing to thermalize the lattice.[22] As a measure of the coupling between various phonons and the impurity, we compute the percentile participation amplitude $\chi_i = \hat{q}\vec{Q}_k/|Q_k|100\%$, where the subscript i = s, l, t identifies the unit vector as the molecular stretch, libration, and center of mass motion, respectively. The computed spectral densities are shown in Fig. 6. As expected, the center of mass motion is most strongly coupled to the acoustic modes, the magnitude peaking near 15 cm^{-1} (due to truncation of the lattice the density below 10 cm^{-1} is not well represented). This coupling channel is clearly ineffective, as evidenced from the T-dependence. The coupling of phonons to the molecular libration is more than an order of magnitude larger than to the internal vibration, with a spectral density that peaks to ~6% around $\omega = 34$ cm^{-1}. The

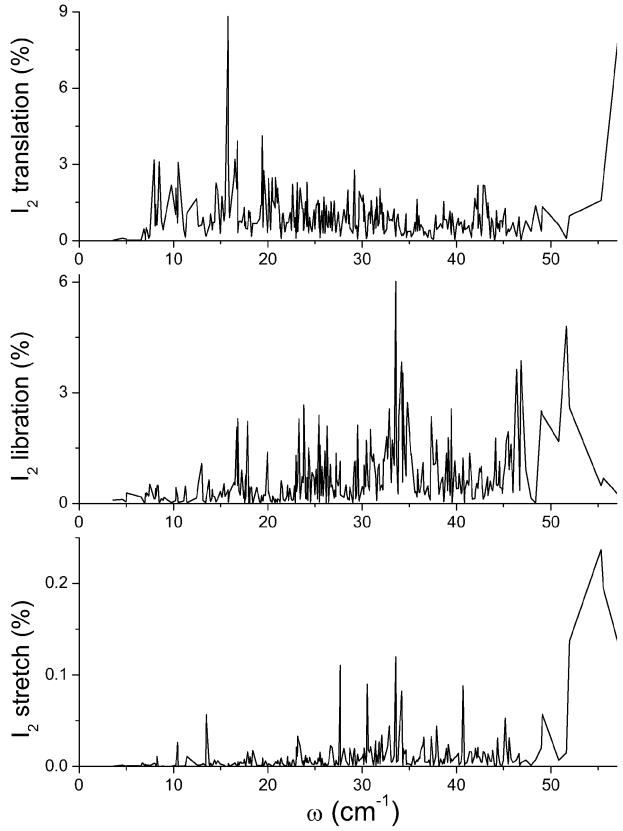

Fig. 6 Decomposition of the normal modes of the doped lattice in terms of percentile participation amplitudes of: (a) molecular stretch, (b) molecular libration, (c) motion of the molecular center-of-mass.

same modes are also among the most strongly coupled to the stretch. As such, the coupling between the molecular vibration and the librational phonons are suggested as the likely channel for dephasing. For a spectral density $\Gamma(\omega)$ that contributes to dephasing the temperature dependence is modified:

$$\gamma(T) = \frac{v}{\tau_1} + \frac{v^2}{\tau_2}\int \mathrm{d}\omega\, n(\omega_k)[n(\omega_k)+1]\Gamma(\omega)^2 \qquad (14)$$

As shown in Fig. 7, the data can be well fit by assuming $\Gamma(\omega)$ centered at $\omega = 34\ \mathrm{cm}^{-1}$, with a width of 3–5 cm^{-1} (the choice of different widths is compensated by the magnitude of τ_2). All of the data in Fig. 4 are combined to generate Fig. 7, by plotting $(\gamma(v, T) - v/\tau_1)v^{-2}$ *versus* T. The width of the distribution may be ascribed to either the distribution of phonons that couple to the molecular vibration, or to the lifetime of the pseudo-local phonon. The accuracy of the T-dependence data is not sufficient to directly extract a spectral density from the experiments.

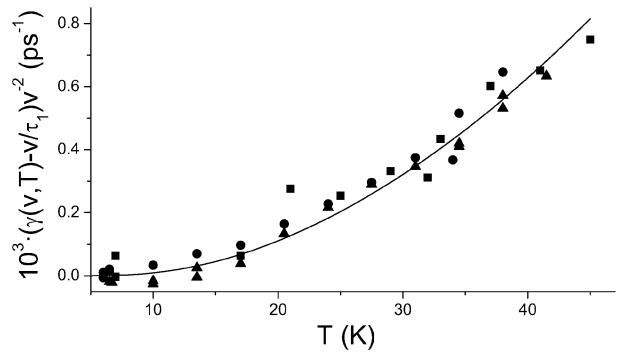

Fig. 7 T-dependence of pure dephasing corrected for v dependence, $v = 8$ (■), 14(●) and 18(▲). The curve is for a Gaussian spectral density centered at $\omega_k = 34\ \mathrm{cm}^{-1}$ and a width of 5 cm^{-1}.

5. Conclusions

I_2 isolated in solid Kr is prototypical of a Morse oscillator trapped in a harmonic bath. This, we establish through the reported time and frequency resolved CARS measurements. Due to the long-lived vibrational coherences, the present time-domain measurements constitute the highest resolution determination of vibrational frequencies of the matrix isolated molecule for $v = 1$–19. The solvated molecular potential up to $E = 3500\ \mathrm{cm}^{-1}$, is well represented as a Morse potential, and its modification is well described as resulting from a local quadratic potential: $V(q) = V_g - k'q^2/2$, where V_g is the gas phase molecular potential and $k' = 2.27 \times 10^3\ \mathrm{cm}^{-1}/\mathrm{Å}^2$. The experiments provide the v-dependent dephasing rates as a function of temperature. In the $T \rightarrow 0$ limit, the vibrational coherence lasts for $1/(2\gamma_v) = 175$ ps ($\sim$1000 periods) for $v = 1$, while for $v = 19$, $1/(2\gamma_v) = 9$ ps ($\sim$50 periods). The linear dependence on vibrational quantum numbers establishes the low temperature decay to be controlled by dissipation, which must be accompanied by the creation of minimally four phonons, and hence is controlled by the quintic coupling between the molecule and the lattice. The quadratic v-dependence of the high temperature decay identifies it as pure dephasing. The observed exponential T-dependence of this process is generally consistent with the model of dephasing *via* pseudo-local phonons.[4] A normal mode analysis suggests that the librations of the molecule act as the principal coupling channel, however, a more rigorous analysis remains quite desirable. We hope that the systematic measurements in this prototype would serve as testing grounds for different theoretical approaches to this fundamental process.

Acknowledgements

This research was made possible through a USAFOSR grant: FA9550-04-1-0186.

References

1 D. W. Oxtoby, *Adv. Chem. Phys.*, 1979, **40**, 1–48.
2 D. W. Oxtoby, *Adv. Chem. Phys.*, 1981, **47**, 487–519.
3 J. L. Skinner, *Annu. Rev. Phys. Chem.*, 1988, **39**, 463–478.
4 J. L. Skinner and D. Hsu, *Chem. Phys.*, 1988, **128**, 35–45.
5 S. Yang, J. Shao and J. Cao, *J. Chem. Phys.*, 2004, **121**, 11250–11271.
6 V. Barsegov and P. J. Rossky, *Chem. Phys.*, 2004, **296**, 103–115.
7 R. D. Coalson and D. G. Evans, *Chem. Phys.*, 2004, **296**, 117–127.
8 Q. Shi and E. Geva, *J. Chem. Phys.*, 2004, **120**, 10647–10658.
9 J. S. Bader, B. J. Berne, E. Pollak and P. Hanggi, *J. Chem. Phys.*, 1996, **104**, 1111–1119.
10 A. Laubereau and W. Kaiser, *Rev. Mod. Phys.*, 1978, **50**, 607–665.
11 T. Elsaesser and W. Kaiser, *Annu. Rev. Phys. Chem.*, 1991, **42**, 83–107.
12 S. Mukamel, *Annu. Rev. Phys. Chem.*, 2000, **51**, 691–729.
13 W. Zinth, H. J. Polland, A. Laubereau and W. Kaiser, *Appl. Phys. B*, 1984, **26**, 77–88.
14 R. Bozio, P. L. Decola and R. M. Hochstrasser, in *Time Resolved Vibrational Spectroscopy*, ed. G. A. Atkinson, Academic Press, New York, 1983.
15 K. Duppen, D. P. Weitekamp and D. A. Wiersma, *J. Chem. Phys.*, 1983, **79**, 5344–5835.
16 J. C. Wright, *Int. Rev. Phys. Chem.*, 2002, **21**, 185–255.
17 S. Mukamel, *Principles of Nonlinear Optical Spectroscopy*, Oxford University Press, New York, 1999.
18 H. Dubost and R. Charneau, *Chem. Phys.*, 1976, **12**, 407–418.
19 I. H. Bachir, R. Charneau and H. Dubost, *Chem. Phys.*, 1993, **177**, 675–692.
20 M. Karavitis, R. Zadoyan and V. A. Apkarian, *J. Chem. Phys.*, 2001, **114**, 4131–4140.
21 M. Karavitis, D. Segale, Z. Bihary, M. Pettersson and V. A. Apkarian, *Low Temp. Phys.*, 2003, **29**, 814–821.
22 M. Karavitis and V. A. Apkarian, *J. Chem. Phys.*, 2004, **120**, 7576–7589.

23 M. Pettersson *et al*., manuscript in preparation.
24 T. Wilhelm, J. Piel and E. Riedle, *Opt. Lett*., 1997, **22**, 1494–1496.
25 E. Riedle, M. Beutter, S. Lochbrunner, J. Piel, S. Schenkl, S. Sporlein and W. Zinth, *Appl. Phys. B*, 2000, **71**, 457–465.
26 C. B. Harris, R. M. Shelby and P. A. Cornelius, *Phys. Rev. Lett*., 1977, **38**, 1415–1419.
27 S. Marks, P. A. Cornelius and C. B. Harris, *J. Chem. Phys*., 1980, **73**, 3069–3081.
28 P. de Bree and D. A. Wiersma, *J. Chem. Phys*., 1979, **70**, 790–801.
29 G. Herzberg, *Spectra of Diatomic Molecules*, van Nostrand Reinhold, New York, 1950.
30 Z. Bihary, R. B. Gerber and V. A. Apkarian, *J. Chem. Phys*., 2001, **115**, 2695–2701.
31 Z. Bihary, M. Karavitis, R. B. Gerber and V. A. Apkarian, *J. Chem. Phys*., 2001, **115**, 8006–8013.
32 J. Wu and J. Cao, *J. Chem. Phys*., 2001, **115**, 5381–5391.
33 A. G. Redfield, *Adv. Magn. Reson*., 1965, **1**, 1–32.
34 D. E. McCumber and M. D. Sturge, *J. Appl. Phys*., 1963, **34**, 1682–1684.

